RESEARCH ARTICLE

Andreas Klügel · Thomas R. Walter ·
Stefanie Schwarz · Jörg Geldmacher

Gravitational spreading causes en-echelon diking along a rift zone of Madeira Archipelago: an experimental approach and implications for magma transport

Abstract Many volcanic rift zones show dikes that are oriented oblique rather than parallel to the morphological ridge axis. We have evidence that gravitational spreading of volcanoes may adjust the orientation of ascending dikes within the crust and segment them into en-echelon arrays. This is exemplified by the Desertas Islands which are the surface expression of a 60 km long submarine ridge in southeastern Madeira Archipelago. The azimuth of the main dike swarm (average = 145°) deviates significantly from that of the morphological ridge (163°) defining an en-echelon type arrangement. We propose that this deviation results from the gravitational stress field of the overlapping volcanic edifices, reinforced by volcano spreading on weak substratum. We tested our thesis experimentally by mounting analogue sand piles onto a sand and viscous PDMS substratum. Gravitational spreading of this setup produced en-echelon fractures that clearly mimic the dike orientations observed, with a deviation of 10°–32° between the model's ridge axis and that of the main fracture swarm. Using simple numerical models of segmented dike intrusion we found systematic changes of displacement vectors with depth and also with distance to the rift zone resulting in a complex displacement field. We propose that at depth beneath the Desertas Islands, magmas ascended

along the ridge to produce the overall present-day morphology. Above the oceanic basement, gravitational stress and volcano spreading adjusted the principal stress axes' orientations causing counterclockwise dike rotation of up to 40°. This effect limits the possible extent of lateral dike propagation at shallow levels and may have strong control on rift evolution and flank stability. The results highlight the importance of gravitational stress as a major, if not dominant factor in the evolution of volcanic rift zones.

A. Klügel (✉) · S. Schwarz
Universität Bremen, Fachbereich Geowissenschaften,
Postfach 330440,
28334 Bremen, Germany
e-mail: akluegel@uni-bremen.de
Tel.: +49-421-2187767
Fax: +49-421-2189460

T. R. Walter
Marine Geology and Geophysics, RSMAS,
University of Miami,
4600 Rickenbacker Causeway,
Miami, FL 33149, USA

J. Geldmacher
IFM-GEOMAR, Leibniz-Institute for Marine Sciences,
Wischhofstr. 1-3,
24148 Kiel, Germany

Introduction

Catastrophic flank collapses of oceanic island volcanoes may cause tsunamis and pose a major natural hazard for coastal zone populations. Of the many factors controlling the stability of volcano flanks, the presence of rift zones is probably the most crucial one because they are the locus of volcano growth where constructive and destructive processes closely interact (Dieterich 1988; Moore et al. 1994; Carracedo 1994; Walter and Schmincke 2002). Rift zones are common on many volcanoes and are characterized by concentration of adjoining cinder cones, normal faults and parallel dike swarms within an elongated area (Fiske and Jackson 1972; Carracedo 1994; Walker 1999). They are underlain by intrusive complexes which may vary in size and position during rift evolution (Walker 1987, 1992). Although difficult to decipher by direct observations or geophysical measurements, knowledge of the internal rift structure is essential for assessing a volcano's eruptive behavior and flank stability.

The explicitness and orientation of dike swarms and eruptive fissures can be used to approximate the direction of the least principal compressive stress σ_3. This is because most dikes are extensional fractures (hydrofractures) and in a homogeneous medium intrude perpendicular to σ_3, as

has been shown by theoretical studies and field observations (e.g. Anderson [1951](#); Gudmundsson [1995](#)). In a rift zone forming an elongated topographic rise, gravitational forces would cause dikes to intrude parallel to the ridge axis (Fiske and Jackson [1972](#)). For such a rift to persist and to accommodate to the emplacement of hundreds or thousands of dikes, there must be a mechanism such as slip on deep faults or on mechanically weak layers in order to relax σ_3 between the injections (Dieterich [1988](#); Borgia [1994](#)). A complex interplay and feedback mechanism between dike intrusions, rift slope and basal fault strength is thus a prerequisite for the formation and growth of volcanic rift zones.

Under certain circumstances, however, dike orientation may differ significantly from the original or primordial direction indicated by rift axes or morphological ridges. This apparent "misorientation" is in many cases the result of regional shear tectonics as observed e.g. on some Azores Islands (Walker [1999](#)), at the Tarawera rift, New Zealand (Nairn and Cole [1981](#)) or at oblique-spreading ridges such as the Reykjanes Peninsula, Iceland (Gudmundsson [2000](#); Clifton and Schlische [2003](#)). Alternatively, it may reflect changes in the local stress field caused by destabilization and collapse of volcano flanks as proposed e.g. for La Palma, Canary Islands (Walter and Troll [2003](#)), or by gravitational forces within a growing complex edifice such as at Mt. Etna (McGuire and Pullen [1989](#)). The dike arrangement within a volcano can also be influenced by stresses induced by neighbouring edifices. Walter ([2003](#)) showed for Tenerife, Canary Islands, that the gravitational spreading of adjacent and overlapping edifices influences the deformation pattern, which may result in the development and configuration of rift zones. Yet the principles and relevance of such a buttressing effect remain largely unexplored. In this paper, we describe an example where gravitational spreading of adjacent volcanic islands may be responsible for the obliquity of a rift's dike swarm relative to the respective ridge axis. Similar situations may be common on volcanic islands worldwide and may strongly affect constructive and destructive processes during volcano evolution.

Geological setting and field observations

Madeira Archipelago comprises the volcanic islands of Porto Santo (14.3–11.1 Ma subaerial age), Madeira (5.3 Ma to <10 ka) and the three Desertas Islands Chao, Deserta Grande and Bugio (5.1–1.9 Ma) (Geldmacher et al. [2000](#); Schwarz et al. [2005](#)). It is located on Cretaceous oceanic crust between magnetic anomalies M4 and M16 (Klitgord and Schouten [1986](#); Roest et al. [1992](#)) and marks the end of a >70 Ma old hotspot chain. The Desertas Islands form the top of a 60 km long submarine ridge, situated on the lower submarine flank of Madeira with a morphological depression between both edifices (Fig. [1](#)). The Desertas ridge is interpreted as either an abandoned rift arm of Madeira (Geldmacher et al. [2000](#)) or a separate volcanic system (Schwarz et al. [2004](#)).
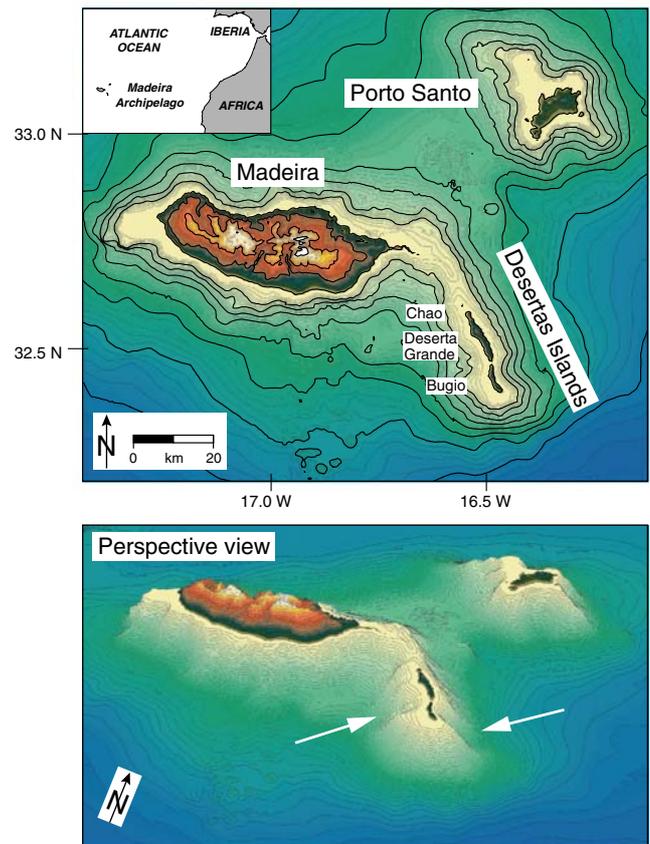

Fig. 1 (**a**) Map of Madeira Archipelago with 100 m contours; bathymetry is based on Smith and Sandwell ([1997](#)) and nautical maps. The islands of Chao, Deserta Grande and Bugio mark the top of the Desertas ridge striking ca. 163° NW-SE. (**b**) Perspective view of the archipelago (3x vertical exaggeration) shows the shape of the Desertas ridge and highlights embayments at the western and eastern flanks as inferred major landslide scarps (*white arrows*)

The Desertas Islands represent the eroded and deeply dissected remnant of a classic rift zone (Schwarz et al. [2005](#)). They consist of local series of lava flows and abundant cinder and tuff cones stacked one on another, that are cut by swarms of steeply dipping dikes (Fig. [2](#)). The dikes crop out along the steep cliffs of Deserta Grande and Bugio but are only locally accessible. Dike thicknesses typically vary between 0.5 and 2 m but can reach up to 10 m. One major dike swarm is readily identifiable in the field by its preferred orientation and by the occurrence of sheeted dikes. Although the strike of the main dike swarm would be expected to parallel the morphological ridge axis (Fiske and Jackson [1972](#)), our measurements along the islands' flanks and crests indicate a significant divergence: 90 per cent of the dikes from the main swarm strike between 120° and 170° NW-SE (average = 145°) and thus clearly deviate from the ridge azimuth of ca. 163° (Fig. [3](#)). The main swarm thus shows counterclockwise rotation relative to the ridge direction. Despite considerable variation, there is no systematic change of this rotation along the 20 km long subaerial ridge (Fig. [3b](#)).

Since the Desertas dikes conspicuously point towards Madeira, we hypothesize that this island is the cause of

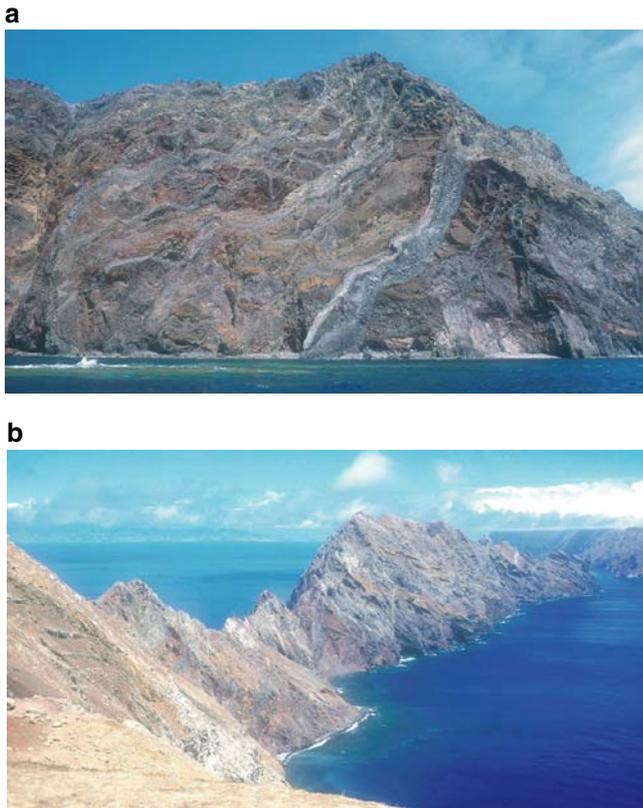**Fig. 2** (**a**) Dike swarm exposed at the western coast of Bugio island. The dikes cut a sequence of tuff and scoria with intercalated lava flows and crop out slightly oblique to the coast line. Height of cliff is about 150 m. (**b**) View from southern Bugio island towards NNE along the Desertas ridge axis. Bugio shows a ragged crest and consists largely of tuff, scoria and local lava flows cut by abundant dikes. *Background* shows the islands of Deserta Grande (*right*, top covered by clouds) and Madeira (*left*)
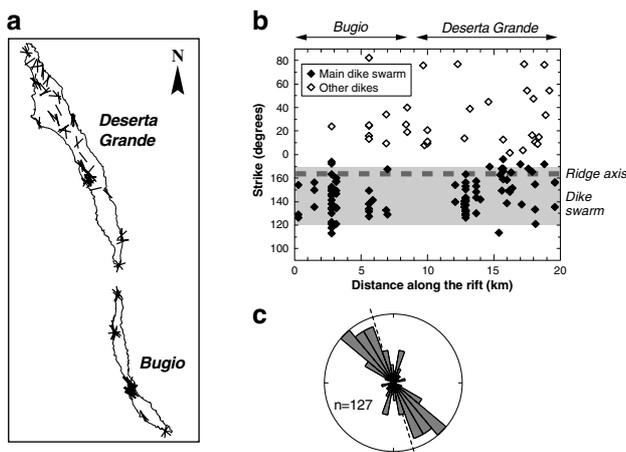

Fig. 3 (**a**) Map of Deserta Grande and Bugio showing the localities of measured dikes. (**b**) Plot of dike azimuth against distance indicates that there is no systematic variation along the Desertas rift. *Dashed line* marks azimuth of the Desertas ridge axis, *gray field* marks range of 90% of the dikes from the main dike swarm. These dikes show a near-Gaussian distribution with average = median = 145°. (**c**) Rose diagram with 10° classes indicates the azimuth of 127 dikes measured on the Desertas Islands; *dashed line* marks the ridge axis. Each data value represents the average of 2 to 28 measurements

the observed dike rotation relative to the ridge axis. An appropriate stress field could result from gravity-driven spreading of Madeira, the lower flank of which underlies the Desertas ridge, because Madeira as well as the Desertas Islands are steep edifices that are prone to gravitational spreading (cf. Merle and Borgia 1996). In order to test our thesis, we carried out analogue experiments to simulate the tectonic situation.

Experimental approach

The analogue experiments account for the following structural units: (A) a ductile layer of prevolcanic continental margin sediments underlying the archipelago, (B) a more competent layer of synvolcanic sediments, and (C) the volcanic edifices. The thicknesses of units (A) and (B) are not known but were estimated based on seismic profiles that were taken near the western Canary Islands (Banda et al. 1992), located 500 km to the south. The profiles indicate two-way travel times of 1–1.5 s for the sedimentary layers between magnetic anomalies M4 and M16 and also near the islands, which converts into thicknesses of 1.0–2.2 km using the wave velocity model of Watts et al. (1997). We thus tentatively assigned a 1 km thickness to unit (A) and a 0.5 km thickness to unit (B), in qualitative agreement with isopach data from Collier and Watts (2001) for the western Canary Islands. The height of the volcanic edifices (C) above the deep sea floor is about 6 km for Madeira and 4.5 km for the Desertas and Porto Santo (Table 1).

Ductile unit (A) was modelled using a ca. 0.5 cm thick layer of viscous PDMS (polydimethylsiloxane) that was placed on a rigid plate. The PDMS has a viscosity of about 3×10^4 Pas and a Newtonian rheology (ten Grotenhuis et al. 2002). The overlying, more brittle unit (B) was simulated using a 0.2–0.3 cm thick layer of dry cohesionless sand (grain size 0.1–0.5 mm) onto which sand piles representing the volcanic edifices were placed (Fig. 4a). This setup resembles those of Merle and Borgia (1996) and Walter (2003), with sand imitating the behaviour of brittle-deforming materials. The sand piles were sprinkled with a thin layer of flour to accentuate the fractures that formed. Although all setups were geometrically similar and care was taken to closely match the topographic relations at Madeira Archipelago (Fig. 1), each experiment was unique in its detailed configuration.

In order to scale the experiments properly, the Buckingham-Π theorem was used according to Merle and Borgia (1996) and Borgia et al. (2000), where five dimensionless numbers $\Pi_1...\Pi_5$ should have similar values for the natural systems and the experiments (Table 1). Initial geometric scaling was 5×10^{-6} for the vertical and 2×10^{-6} for the horizontal dimensions, i.e., 1 km in nature was scaled in the experiments to 0.5 cm vertical and 0.2 cm horizontal for the islands as well as the distances between them. We note that the initial vertical exaggeration in the experiments increased the edifices' Π_1 values ("potential instability"; Borgia et al. 2000) and thus their tendency to spread (Fig. 5), but it had no noticeable influence on the

Table 1 Comparison of scaling parameters of the natural systems and the experiments

	Variable	Description	Desertas/Madeira	Experiments	Unit
Geometric scaling	S_1	Thickness of brittle substratum	500	0.0025	m
	S_2	Thickness of weak substratum	1000	0.005	m
	H	Height of volcanic edifice above deep seafloor	4500/6000	0.023/0.030[a]	m
	D	Diameter of short axis of volcanic edifice (at 2500 m depth contour)	32000/56000	0.064/0.112[a]	m
Kinematic and dynamic scaling	ρ_1	Density of volcanic cone	2700	1400	kg m^{-3}
	ρ_2	Density of substratum	2500	1200	kg m^{-3}
	ν	Viscosity of weak substratum	5E+18	30000	Pa s
	μ	Internal friction coefficient	0.6	0.6	
	g	Gravity acceleration	9.8	9.8	m s^{-1}
	t	Time span of deformation	3.2E+13 (1 mill. years)	86400 (1 day)	s
					Π* ratio[b]
Buckingham numbers	$\Pi_1 = 2H/D$	Potential instability	0.28/0.21	0.70/0.54[a]	0.4
	$\Pi_2 = S_1/H$	Intrinsic strength of substratum	0.08/0.11	0.08/0.11	1
	$\Pi_3 = S_1/S_2$	Intrinsic weakness of substratum	0.50	0.50	1
	$\Pi_4 = \rho_1/\rho_2$	Volcano floating potential	1.08	1.17	0.93
	$\Pi_5 = (\rho_1 g H t)/\nu$	Process rate	1524/2032	889/1185	1.71

[a]Initial values; the final Π_1 value approaches that of the real systems (see text for details)

[b]The Buckingham ratios Π* are defined by $\Pi_{\text{real volcano}}$ divided by $\Pi_{\text{experiment}}$ and approach 1 where scaling is preserved

Fig. 4 (**a**) Sketch of basic experimental setup. (**b**) Result of experiment TW2 after 6 h of spreading showing fractures oblique to the ridge axis (*dashed line*). (**c**) Detailed view of (**b**). (**d**) Result of experiment MAD3 after 21 h showing fractures and a pronounced graben oblique to the Desertas ridge axis (*dashed line*) as well as grabens along the long axis of Madeira and between Madeira and Porto Santo. (**e**) Same view as (**d**) buth with sand removed. The visible PDMS layer shows elongated diapir-like protrusions indicating regions of major expansion
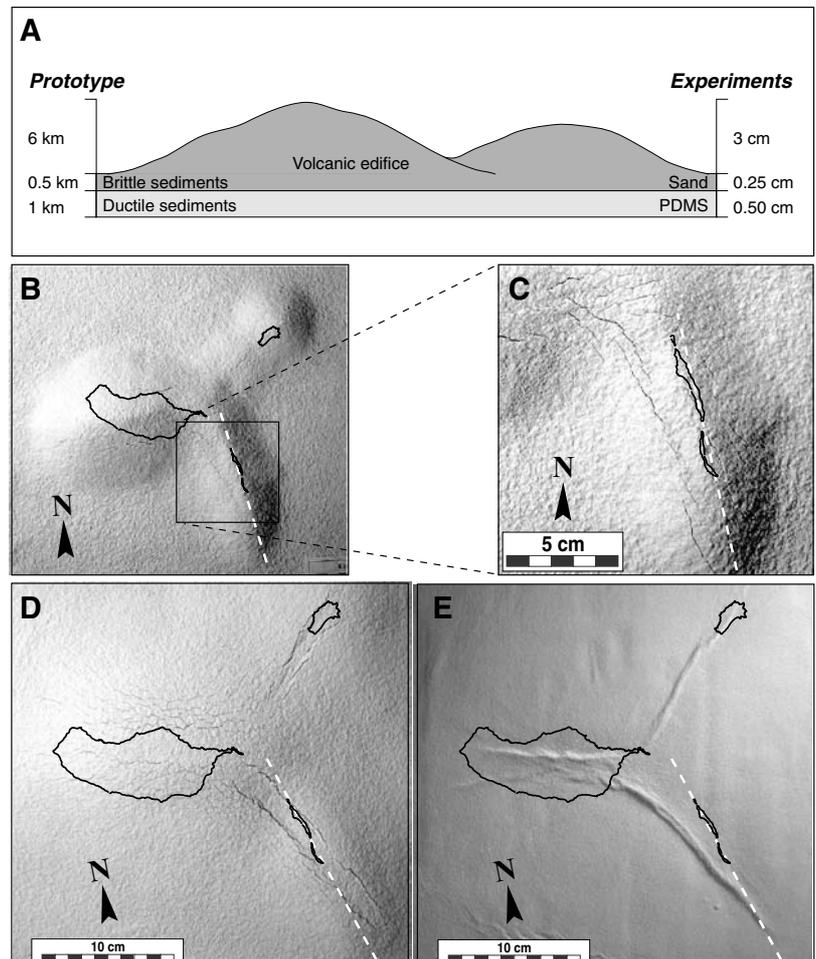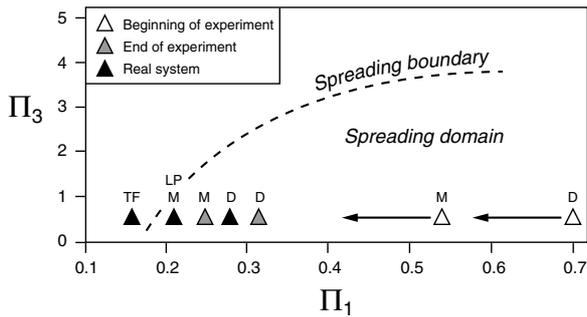
Fig. 5 Plot of Π_1 (potential instability) versus Π_3 (intrinsic substratum weakness) redrawn after Merle and Borgia (1996). An experimentally derived boundary separates a spreading from a non-spreading domain. Madeira (*M*) and the Desertas Islands (*D*) have a tendency to spread but are close to a stable configuration. Data for Tenerife (*TF*; Walter 2003) and La Palma (*LP*) where pronounced rift zones also exist are shown for comparison. The initial vertical exaggeration of the experiments is reflected by their increased Π_1 values, which approach those of the real islands towards the end of an experiment (indicated by *arrows*) where a stable configuration is reached

resulting structures because the direction of motion is determined by the topographic relations rather than the basal slope. During experimental run, the Π_1 values of the model edifices decreased when they spread and approached those of the islands (Fig. 5) so that horizontal and vertical scaling were almost equal at the end of deformation. The other four Π values are similar in nature and in the experiments (expressed in Table 1 by Π^* ratios close to unity) indicating that kinematic and dynamic scaling are preserved. The Π_5 value ("process rate"), however, comprises some uncertainty because the time span of deformation is not known for the real volcanoes. The values given in Table 1 are based on the observation that the bulk of the subaerial Desertas edifice was constructed in less than 2 Ma (Geldmacher et al. 2000; Schwarz et al. 2005) and that most of the spreading in the experiments occurred during the first 24 h.

Experimental results

Despite some variations in overall topography and thicknesses of the layers, all experiments gave qualitatively identical results. About one hour after emplacement, the sand piles developed extensional cracks and normal faults at the surface as a result of gravitational spreading on the viscous substratum (Fig. 4b, c). Crack segments developed along the morphological ridges and diverged radially at the unbuttressed end of the ridge. As spreading continued, three main grabens formed along the Madeira and Desertas ridge axes and between Porto Santo and Madeira converging in the east of Madeira (Fig. 4d, e). The resulting structures, therefore, have some resemblance to the triaxial rift model of Walter (2003) although the topographic situation is different. At the end of the experiments, the observed elongation of the edifices' short axes was 10–25% and the flattening was 35–50%.
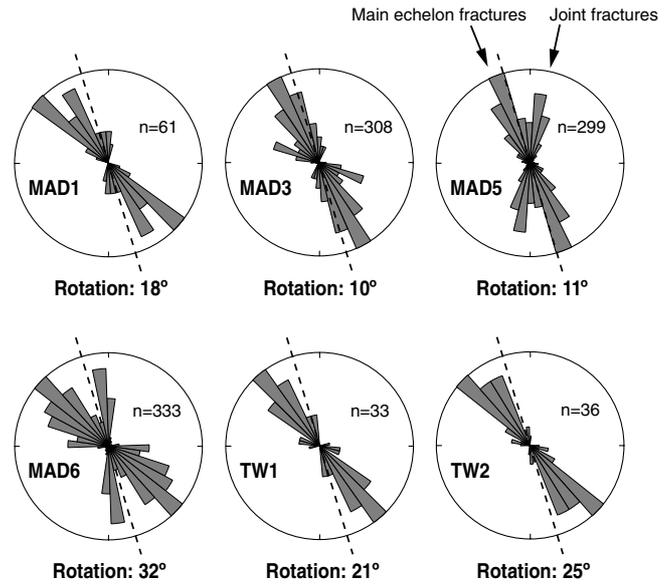

Fig. 6 Rose diagrams with $10°$ classes indicating azimuth of fractures obtained in experiments TW1, TW2, MAD1, MAD3, MAD5 and MAD6; *n* denotes number of fractures measured. Note the good agreement between experimental data and field measurements (Fig. 3c). The indicated rotation is the angle between ridge axis (*dashed line*) and average strike of the main fracture swarm

All experiments show that grabens and main fractures along the modelled Desertas ridge do not parallel its long axis but are rotated counterclockwise (Fig. 6). The fractures are thus arranged in an en-echelon type fashion implying a left-lateral strike-slip deformation type. The orientation of the fractures is roughly constant along the ridge except for areas in close proximity to Madeira. A statistical analysis of fracture orientations shows that they mimic the dike orientations observed in nature well (Figs. 3 and 6). The deviation between the models' ridge axis and the average azimuth of the main fracture swarm ranges from $10°$ to $32°$, which is in agreement with that observed at the Desertas ($18°$). This is a remarkable result considering that all fractures of the experimental ridges are included in the data, whereas at the Desertas ridge only the uppermost (i.e. subaerial) part was accessible for field measurements. Some experiments additionally show a subordinate group of fracture orientations at an angle of $30°–40°$ to the main swarm (e.g., MAD5 and MAD6). This group reflects joint fractures linking the echelon segments and is also observed in the dike pattern on the Desertas Islands (Fig. 3). Despite qualitative agreement of all experimental results, the distribution of fracture orientations—and hence the local stresses–depended strongly on the actual geometric configuration.

We emphasize that we did not observe a systematic change in fracture orientations during the course of an experiment. Fractures that formed during the first hours merely became wider as spreading of the sand piles continued and were representative for the orientation of the main fracture swarm. This implies that (1) there is little change in the orientation of σ_3 during spreading, and (2)

the experimental results are essentially independent of run duration. As a consequence, the uncertainty in scaling the process rate (Π_5 value) as discussed above does not affect our results and interpretations.

After removal of the sand piles, the ductile bottom layer revealed elongated diapir-like protrusions beneath the ridges indicating considerable extension at their base (Fig. 4e). The orientation of these protrusions is subparallel to the surface fractures implying that there is little change in the orientation of σ_3 along the height of the ridges.

Numerical modeling

The strike of a rift zone and of its individual dikes usually parallels the direction of the respective topographic ridge (cf. Fiske and Jackson 1972; Dieterich 1988). The direction of displacement and flank deformation is accordingly thought to be normal to the rift zone. We now show that this does not apply to the en-echelon dikes of a Desertas-type rift zone. Based on (1) measured dike orientations on the Desertas Islands and (2) development of en-echelon type fractures in the analogue models, we assume that dike orientations at depth differ from dike orientations closer to the surface. Dike orientation within the oceanic crust is presumably collinear and parallel to the topographic ridge, whereas dike orientation within the ridge itself and closer to the surface is en-echelon. This discrepancy must affect the mechanism of intrusive widening (dilatation) of the Desertas Islands and the development of flank instability.

In simple numerical models we tested the influence of dike orientation along the Desertas rift zone. We simulated en-echelon dislocation segments in order to study the displacement caused by en-echelon dikes close to the surface of the Desertas Islands, and we compared these models to a collinear dislocation model which simulates rifting in deeper levels.

For the calculations the elastic modelling formulae of Poly3d (Thomas 1993) was used. The three-dimensional boundary element numerical code is based on the equations of linear elastic fracture mechanics for homogeneous and isotropic materials (Comninou and Dunders 1975). In the models, individual dike segments were discretized into triangular elements acting as planar dislocations of constant displacement discontinuity. The combination of these dislocation elements allows to simulate almost any dislocation geometry. We discretized the boundaries of tensional cracks (i.e., dikes) that were embedded in a linear-elastic half-space material. A Young's modulus of $E=50$ GPa and a Poisson's ratio of $v=0.25$ were assigned as mechanical properties typical of volcanoes (e.g. Okubo et al. 1997).

We defined a 1 m uniform normal displacement at each dislocation plane, which refers to 1 m dike opening as the only type of loading in the models; no regional stress field was applied. From 0–5 km depth (the volcanic edifice) we defined eight en-echelon "dikes", and from 5 to 10 km depth (the oceanic crust) we defined one collinear "dike". We computed the displacement at the en-echelon dike segments (Fig. 7a) and at the collinear dike (Fig. 7b) by using horizontal sections through 2.5 km and 7.5 km depth.

The results of the models indicate that segmented dike intrusion in an en-echelon pattern results in curved displacement vectors. At some distance to the rift zone, the direction of displacement is normal to the ridge axis. Close to the rift, however, the displacement field is rotated such that the displacement direction is oblique to the topographic ridge (Fig. 7a). Nearby crack segments thus act as a single crack in the far field (cf. Sneddon and Lowengrub 1969). This behaviour contrasts with the situation near the collinear dislocation plane at depths greater than 5 km. Here, the displacement vectors are perpendicular to the direction of the rift zone (Fig. 7b) as has been described for Hawaiian volcanoes (Dieterich 1988; Borgia 1994). Thus, the displacement of collinear rifting at depth fundamentally differs from the displacement along en-echelon dike patterns closer to the surface. The results indicate complex rotation of displacement vectors: 1) displacement is normal to the rift zone at depth and becomes oblique at shallow levels (rotation in a vertical plane), 2) displacement is normal away from the rift zone and becomes oblique in proximity to the rift (rotation in the horizontal plane). This rotation of displacement vectors represents a novel case postulated for rift zones of oceanic island volcanoes and may have affected flank stability at the Desertas Islands (Fig. 7c).

Discussion

In analogue experiments, we studied the effect of gravitational spreading of adjacent volcanic ridges on fracture distribution. The morphology of Madeira Archipelago defined the prototype, which was simulated by appropriate piles of sand. A mechanically weak layer was defined only at the base of the experimental setup where we simulated a layer of viscous substratum between the stiff oceanic crust and the volcanoes. On this layer, the sand cones deformed due to their load and fractures developed at the surface. All experiments showed good agreement between simulated fracture arrangements and measured dike trends. This allows us to make some robust inferences on stress distribution and magma transport.

We propose that the observed discrepancy between dike and ridge orientations reflects a particular scheme of volcano spreading on weak pre-volcanic sediment. At an isolated ridge where flanks can spread freely to accommodate to dike emplacement, injected dikes are oriented ridge-parallel reflecting a direction of σ_3 normal to the ridge axis (Fiske and Jackson 1972; Dieterich 1988). At the Desertas ridge, however, spreading and mutual buttressing of the overlapping Madeira and Desertas edifices adjusted the principal stress axes' orientation. This resulted in a left-lateral stress component at shallow levels that caused σ_3 to rotate counterclockwise and dikes to strike oblique to the ridge axis (Fig. 8a).

Figure 8b illustrates this scenario. At depth, within the oceanic crust and/or uppermost mantle, there must have

Fig. 7 Results of numerical models showing intrusive widening and displacement vectors at (**a**) 2.5 km depth as caused by an array of en-echelon dikes, and (**b**) at 7.5 km depth as caused by a single collinear dike. *Colors* indicate the amount of displacement normal to the rift axis. The shallow displacement field is strongly curved and differs markedly from the deep one showing ridge-normal displacement vectors. (**c**) Relation between the orientation of presumed landslide scarps and the predicted shallow displacement vectors
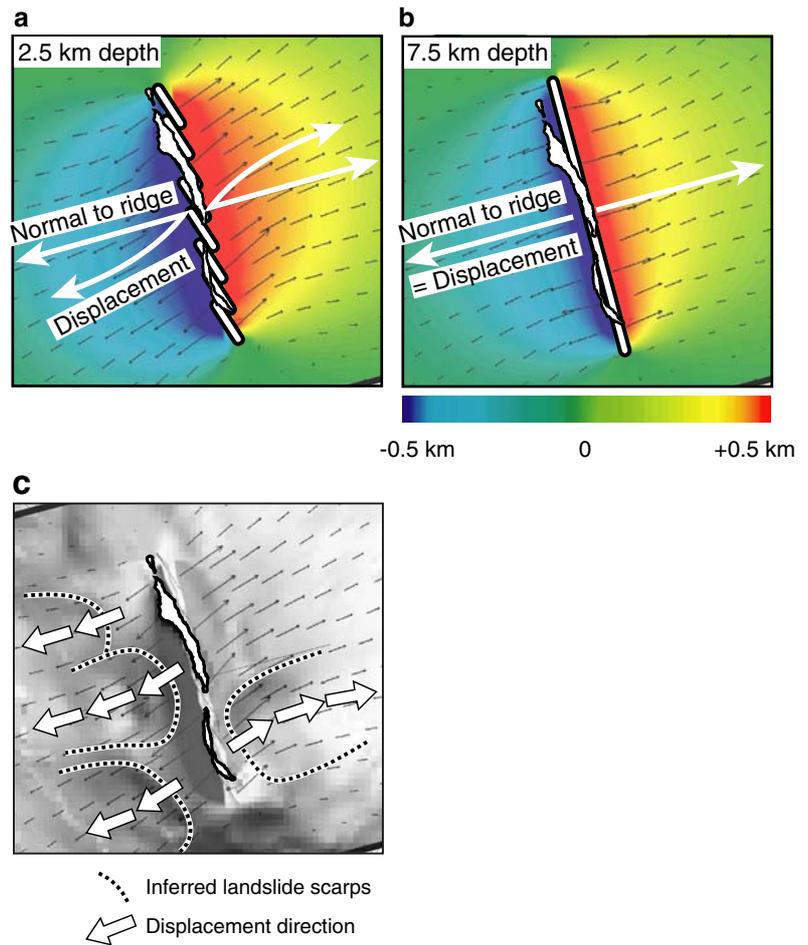
been a regional stress field or a zone of weakness such that σ_3 was normal to the Desertas ridge. Ascending dikes were thus oriented parallel to the ridge axis and produced the present ridge morphology by intrusion and extrusion of magma. Within the Desertas edifice, however, the direction of σ_3 was about $20°$ oblique to the normal direction which caused counterclockwise rotation of ascending dikes. This rotation resulted either in en-echelon arrangement of individual dikes or in the breakdown of ascending parent dikes into en-echelon segments (Pollard et al. 1982; Fig. 8b). Both scenarios are principally possible and can account for the observed dike arrangement, but they are indistinguishable at the Desertas Islands because most of the inferred rotation occurs at depth.

Our model raises the question whether the postulated rotation of ascending dikes occurs (1) within the brittle Desertas edifice or (2) within the ductile layer of weak prevolcanic sediments underlying it. We suspect that the ductile layer decoupled the deep regional stress from the shallow gravity-controlled stress and that option (2) is therefore more plausible. If this were the case, our model implies that pronounced dike rotation of about $20°$ occurred close to the mechanically weak sediments in the substratum. Apart from causing dike rotation, this sedimentary layer overlying the stiff oceanic crust is a likely stress barrier to arrest ascending dikes (Gudmundsson 2002). Our

experiments also appear to support option (2) because the elongated diapirs of ductile substratum beneath the model ridge run parallel to the surface fractures and grabens (Fig. 4d, e). This suggests similar directions of σ_3 at the top and bottom of the ridge. Nevertheless, we point out that both options (1) and (2) result in similar near-surface structures and cannot be distinguished from each other by field observations.

According to Merle and Borgia (1996), gravitational spreading of Madeira and the Desertas Islands is indeed predicted based on the islands' Π values (Table 1). In the $\Pi_1 - \Pi_3$ diagram (Fig. 5), both islands plot in the spreading domain near the spreading boundary which means that they are now close to a stable configuration. During the time of Desertas volcanism, however, their height/diameter ratio Π_1 - and hence their tendency to spread—was higher and the slopes were steeper than today (Schwarz et al. 2005). Strong erosion has since reduced the islands' height and produced volcaniclastic aprons thereby reducing Π_1 to the present-day value.

The layer of ductile prevolcanic sediments underlying the Desertas Islands is responsible not only for the spreading of the islands and the inferred rotation of the main dike swarm. This layer is probably also the horizon where lateral flank slip along deep faults occurs, a prerequisite for repeated dike intrusion and rift growth (Dieterich 1988). We
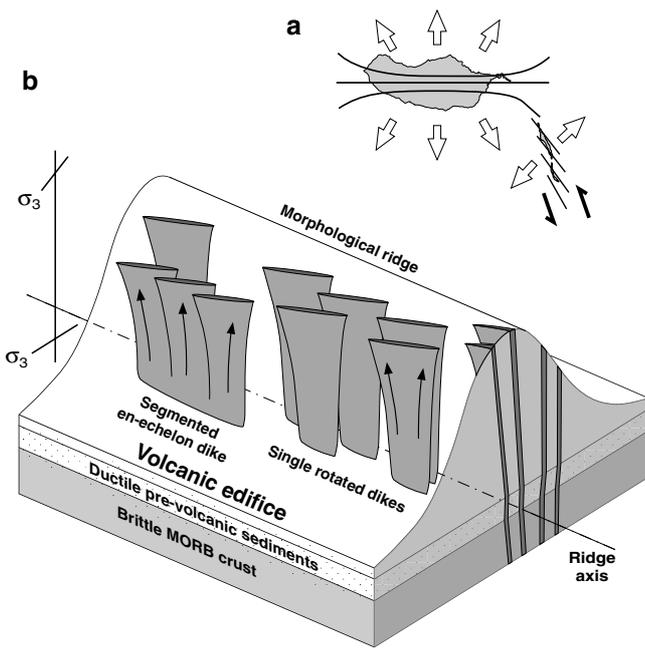
Fig. 8 (**a**) Simple sketch of potential dike directions indicates how spreading of Madeira (*open arrows*) causes a sinistral stress component and dike rotation at the Desertas Islands (*solid arrows*). (**b**) Sketch of dike rotation and en-echelon arrangement within the Desertas ridge (not to scale). Because of changing orientation of the principal stress axis σ_3, ascending dikes rotate counterclockwise around a vertical axis or become segmented. Both scenarios result in en-echelon arrangements of the dikes at the ridge surface.

hypothesize that the existence of this layer is the decisive factor for the formation of the highly elongated Desertas rift zone and its persistence for more than two million years, which is the time during which most of the subaerial edifice was built (Schwarz et al. 2005). A similar situation exists at the western Canary Islands where rift zones are more common and more pronounced than at the eastern islands (Carracedo 1994). This observation coincides with strong changes in substratum (Watts et al. 1997; Collier and Watts 2001): as the continental margin becomes closer and the islands become older from west to east, the thickness of ductile sediments increases and that of more competent sediments increases even more so, which results in increased Π_2 and Π_3 and probably in a reduced spreading potential.

The hallmark of our model is that local gravitational forces rather than regional tectonics control the rotation of the Desertas Islands' main dike swarm and produce the en-echelon arrangement observed. This implies that during growth of the rift zone and formation of the pronounced Desertas ridge, gravitational stress progressively dominated over regional stress causing rotation of σ_3 at depth and with time. This scenario is similar to the situation proposed for Etna volcano (McGuire and Pullen 1989). Another example for gravity-controlled rotation and segmentation of dikes is Mauna Loa volcano (Hawaii) where dikes are injected from a shallow summit reservoir into rift zones. In 1975 and 1984, such dikes propagated laterally up to 20 or

more kilometres into the rift zones. Associated surface fractures developed in segments and lava fountains migrated in series of south-stepping echelon fissures into the northeast rift zone (Lockwood et al. 1987). The approximate dike obliquity relative to the rift axis is $<10°$ and thus significantly less than at the Desertas Islands ($<40°$, average 19°, Fig. 3). The en-echelon dikes at Mauna Loa may reflect the shallow gravitational stress regime of the irregularly shaped and deforming edifice.

In contrast, dike rotation at many other localities such as Sao Miguel and Pico (Azores), Tutuila (Samoa), Oahu (Hawaii) and the Reykanes Peninsula (Iceland) results from oblique extension due to regional tectonics (Gudmundsson 1987; Clifton and Schlische 2003). For example, the Laki 1783 and Eldgja 934 eruptions on Iceland produced 20–40 km long rows of craters reflecting lateral fissure propagation from central volcanoes. These crater rows are segmented in a sinistral en-echelon fashion probably as a result of extensional tectonics oblique to the rift zone (Gudmundsson 1990, 2000; Thodarson and Self 1993; Jónsson et al. 1997). Tensional en-echelon surface fractures are traditionally thought to propagate from the surface downwards, however, a new conceptual model developed on Iceland suggests upward propagation from a main fracture at depth and echelon-type segmentation closer to the surface (Grant and Kattenhorn 2004). Based on our experimental and numerical modelling we also suggest dike segmentation to occur within the upper crust beneath the Desertas Islands.

It should be noted that dike segmentation in general is the rule rather than the exception. Segmented dikes are ubiquitous in lateral and vertical sections and can reflect changes in σ_3 orientation, mechanical heterogeneities or crack-to-crack interaction (e.g. Gudmundsson 2002). We point out, however, that the occurrence of en-echelon arrangements relative to a ridge axis does not necessarily indicate that one or more individual dikes have become segmented at depth. As shown in Fig. 8b, rotation of individual dikes around subvertical axes during upward propagation can also result in en-echelon type geometry without any segmentation to occur. The occurrence of sheeted en-echelon dikes such as on the Desertas Islands may be a good indicator for such a scenario, but the actual mechanism may be difficult to reconstruct. In contrast, simultaneous volcanic activity at en-echelon fissures as during the 1783 Laki eruption on Iceland clearly implies dike segmentation (Thodarson and Self 1993; Gudmundsson 1995).

Our results have implications for magma migration and evolution of ridge-forming rift zones. If feeder dikes are oblique to the ridge as suggested for the Desertas rift zone, shallow magma transport over tens of kilometres along-rift as inferred for Hawaiian rift zones can be ruled out. If oblique dikes propagated laterally, they would tend towards the ridge flanks, which would ultimately increase the number of flank eruptions, re-organize the rift system and change the ridge morphology. Since this is not observed at the Desertas ridge, we conclude that lateral magma transport at shallow levels only played a minor role. This conclusion agrees with the inferred absence of shallow

magma reservoirs from which dikes could emanate within the Desertas edifices (Schwarz et al. 2004). In contrast, lateral magma transport is highly relevant on Iceland and Mauna Loa where the observed en-echelon arrangements suggest major dike segmentation to occur at shallow levels, either from a main fracture (or magma chamber) at depth (cf. Grant and Kattenhorn 2004) or above a depth of dominantly lateral magma flow.

The observed obliquity of the main dike swarm relative to the ridge axis places constraints on the internal rift structure (Fig. 8) and may affect flank stability, because flank displacement during intrusion of en-echelon dikes is more complex than that of ridge-parallel intrusions (Fig. 7). The intrusion of dikes up to 10 m thick clearly resulted in considerable movement within the Desertas flanks. In particular, we suspect that oblique rifting introduced strike-slip or oblique-slip faults (cf. Clifton and Schlische 2003) that may have destabilized the edifice and may have promoted wall collapse. We note that the Desertas ridge shows deep-reaching embayments with lateral scarps (Fig. 1b) which strongly suggest that large flank collapses had occurred in the past. One may only speculate, however, whether these collapses were facilitated by the inferred dike obliquity and rotation of the displacement vectors discussed above.

Concluding remarks

The Desertas rift zone of Madeira Archipelago documents that long-term oblique rifting can occur without the existence of regional shear tectonics. Prolonged local shear stress can similarly produce an en-echelon arrangement of successively intruding dikes. A likely mechanism to cause local shear stress is gravitational spreading of adjoining volcanic edifices on weak substratum. The consequence is a depth-dependent orientation of the least compressive stress σ_3 causing rotation of ascending dikes around a vertical axis. This model is confirmed by analogue experiments yielding fracture orientations oblique to the ridge axis. The respective dike orientations differ from that expected from a simple ridge which has implications for rift growth and flank stability. A simple numerical model predicts a complex displacement field during oblique dike intrusion that may have a destabilizing effect of the ridge flanks. Our results suggest that gravitational stress and related spreading are major, if not dominant factors in the evolution of volcanic rift zones.

References

Anderson EM (1951) The dynamics of faulting and dyke formation with applications to Britain. Oliver and Boyd, London, 206 pp

Banda E, Ranero CR, Danobeitia JJ, Rivero A (1992) Seismic boundaries of the eastern Central Atlantic Mesozoic crust from multichannel seismic data. Geol Soc Am Bull 104:1340–1349

Borgia A (1994) Dynamic basis of volcanic spreading. J Geophys Res 99(B9):17791–17804

Borgia A, Delaney P, Denlinger RP (2000) Spreading volcanoes. Ann Rev Earth Planet Sci 28:539–570

Carracedo JC (1994) The Canary Islands: an example of structural control on the growth of large ocean-island volcanoes. J Volcanol Geotherm Res 60:225–241

Clifton A, Schlische R (2003) Fracture populations on the Reykjanes Peninsula, Iceland: Comparison with experimental clay models of oblique rifting. J Geophys Res 108(B2):2074, doi:10.1029/2001JB000635

Collier JS, Watts AB (2001) Lithospheric response to volcanic loading by the Canary Islands: constraints from seismic reflection data in their flexural moat. Geophys J Int 147:660–676

Comninou MA, Dunders J (1975) The angular dislocation in a half-space. J Elasticity 5:203–216

Delaney PT, Pollard DD (1981) Deformation of host rocks and flow of magma during growth of minette dikes and breccia-bearing intrusions near Ship Rock, New Mexico. US Geol Surv Prof Pap 1202:61

Dieterich JH (1988) Growth and persistence of Hawaiian volcanic rift zones. J Geophys Res 93(B5):4258–4270

Fiske RS, Jackson ED (1972) Orientation and growth of Hawaiian volcanic rifts: the effect of regional structure and gravitational stresses. Proc R Soc Lond A 329:299–326

Geldmacher J, Bogaard Pvd, Hoernle KA, Schmincke HU (2000) Ar age dating of the Madeira Archipelago and hotspot track (eastern North Atlantic). Geochemistry, Geophysics, Geosystems 1: Paper number 1999GC000018

Grant JV, Kattenhorn SA (2004) Evolution of vertical faults at an extensional plate boundary, southwest Iceland. J Struct Geol 26:537–557

Gudmundsson A (1987) Geometry, formation and development of tectonic fractures on the Reykjanes Peninsula, Southwest Iceland. Tectonophysics 139:295–308

Gudmundsson A (1990) Dyke emplacement at divergent plate boundaries. In: Parker AJ, Rickwood PC, Tucker DH (eds) Mafic dykes and emplacement mechanisms. Proc Int Dyke Conf 2:47–62

Gudmundsson A (1995) The geometry and growth of dykes. In: Baer G, Heimann A (eds) Physics and chemistry of dykes. Balkema, Rotterdam, Brookfield, pp 23–34

Gudmundsson A (2000) Dynamics of volcanic systems in Iceland: Example of tectonism and volcanism at juxtaposed hot spot and mid-ocean ridge systems. Ann Rev Earth Planet Sci 28:107–140

Gudmundsson A (2002) Emplacement and arrest of sheets and dykes in central volcanoes. J Volcanol Geotherm Res 116:279–298

Jónsson S, Einarsson P, Sigmundsson F (1997) Extension across a divergent plate boundary, the Eastern Volcanic Rift Zone, south Iceland, 1967–1994, observed with GPS and electronic distance measurements. J Geophys Res 102:11913–11929

Klitgord KD, Schouten H (1986) Plate kinematics of the Central Atlantic. In: Vogt PR, Tucholke BE (eds) The geology of North America, vol. M, The Western North Atlantic Region. Geological Society of America, pp 351–378

Lockwood JP, Dvorak JJ, English TT, Koyanagi RY, Okamura AT, Summers ML, Tanigawa WR (1987) Mauna Loa 1974–1984 A decade of intrusive and extrusive activity. In: Decker RW, Wright TW, Stauffer PH (eds) Volcanism in Hawaii, 2. US Geol Surv Prof Paper 1350, pp 537–570

McGuire W, Pullen AD (1989) Location and orientation of eruptive fissures and feeder dykes at Mount Etna; Influence of gravitational and regional tectonic stress regimes. J Volcanol Geotherm Res 38:325–344

Merle O, Borgia A (1996) Scaled experiments of volcanic spreading. J Geophys Res 101:13805–13817

Moore JG, Normark WR, Holcomb RT (1994) Giant Hawaiian landslides. Ann Rev Earth Planet Sci 122:119–144

Nairn IA, Cole JW (1981) Basalt dikes in the 1886 Tarawera rift. New Zeal Jour Geol Geophys 24:585–592

Okubo P, Benz HM, Chouet BA (1997) Imaging the crustal magma sources beneath Mauna Loa and Kilauea, Hawaii. Geology 25:867–870

Pollard DD, Segall P, Delaney PT (1982) Formation and interpretation of dilatant echelon cracks. Geol Soc Am Bull 93:1291–1303

Roest WR, Danobeitia JJ, Verhoef J, Collette BJ (1992) Magnetic anomalies in the Canary Basin and the Mesozoic evolution of the Central North Atlantic. Mar Geophys Res 14:1–24

Schwarz S, Klügel A, Wohlgemuth-Ueberwasser C (2004) Melt extraction pathways and stagnation depths beneath the Madeira and Desertas rift zones (NE Atlantic) inferred from barometric studies. Contrib Mineral Petrol 147:228–240

Schwarz S, Klügel A, Bogaard Pvd, Geldmacher J (2005) Internal structure and evolution of a volcanic rift system in the eastern North Atlantic: the Desertas rift zone, Madeira archipelago. J Volcanol Geotherm Res 141:123–155

Smith WHF, Sandwell DT (1997) Global sea floor topography from satellite altimetry and ship depth soundings. Science 277:1956–1962

Sneddon IN, Lowengrub M (1969) Crack problems in the classical theory of elasticity. Wiley, New York

Thodarson T, Self S (1993) The Laki (Skaftár Fires) and Grímsvötn eruptions in 1783–1785. Bull Volcanol 55:233–263

Thomas A (1993) Poly3D: A Three-Dimensional, Polygonal Element, Displacement Discontinuity Boundary Element Computer Program with Applications to Fractures, Faults, and Cavities in the Earth's Crust. M.S. thesis Thesis, Stanford University, CA

Walker GPL (1987) The dike complex of Koolau volcano, Oahu: Internal structure of a Hawaiian rift zone. In: Decker RW, Wright TW, Stauffer PH (eds) Volcanism in Hawaii, 2. US Geol Surv Prof Paper 1350, pp 961–993

Walker GPL (1992) "Coherent intrusion complexes" in large basaltic volcanoes - a new structural model. J Volcanol Geotherm Res 50:41–54

Walker GPL (1999) Volcanic rift zones and their intrusion swarms. J Volcanol Geotherm Res 94:21–34

Walter TR (2003) Buttressing and fractional spreading of Tenerife, an experimental approach on the formation of rift zones. Geophys Res Lett 30(6):1296 doi:10.1029/2002GL016610

Walter TR, Schmincke HU (2002) Rifting, recurrent landsliding and Miocene structural reorganization on NW-Tenerife (Canary Islands). Int J Earth Sci 91:615–628

Walter TR, Troll VR (2003) Experiments on rift zone evolution in unstable volcanic edifices. J Volcanol Geotherm Res 127:107–120

Watts AB, Peirce C, Collier J, Dalwood R, Canales JP, Henstock TJ (1997) A seismic study of lithospheric flexure in the vicinity of Tenerife, Canary Islands. Earth Planet Sci Lett 146:431–447